PHYSICAL REVIEW D **72,** 063504 (2005)

Can the initial singularity be detected by cosmological tests?

Marek Szydłowski* and Włodzimierz Godłowski
Astronomical Observatory, Jagiellonian University, Kraków, Poland

Adam Krawiec
Institute of Public Affairs, Jagiellonian University, Kraków, Poland

Jacek Golbiak
Department Philosophy of Nature and Philosophy of Natural Sciences, Catholic University of Lublin, Lublin, Poland
(Received 20 June 2005; published 6 September 2005)

In this paper, we raised the question of whether initial cosmological singularity can be proven by cosmological tests. The classical general relativity theory predicts the existence of singularity in the past if only some energy conditions are satisfied. On the other hand, the latest quantum gravity applications to cosmology suggest the possibility of avoiding the singularity and replacing it with a bounce. Bounce is the moment in the evolution of the Universe when the Universe's size is minimum. Therefore the existence of observationally detected bounce in the Universe's past could indicate the validity of the loop quantum gravity hypothesis and nonexistence of initial singularity which is present in the classical ΛCDM. We investigated the bouncing model described by the generalized Friedmann-Robertson-Walker equation in the context of the observations of the currently accelerating universe. The distant type Ia supernovae data are used to constrain the bouncing evolutional scenario where the square of the Hubble function H^2 is given by the formula $H^2 = H_0^2[\Omega_{m,0}(1+z)^m - \Omega_{n,0}(1+z)^n]$, where $\Omega_{m,0}$, $\Omega_{n,0} > 0$ are density parameters and $n > m > 0$. In this paper are shown that, on the basis of the SNIa data, standard bouncing models can be ruled out at the 4σ confidence level. After adding the cosmological constant to the standard bouncing model (the extended bouncing model), we obtained as the best fit that the parameter $\Omega_{n,0}$ is equal to zero which means that the SNIa data do not support the bouncing term in the model. The bouncing term is statistically insignificant on the present epoch. We also demonstrated that BBN offers the possibility of obtaining stringent constraints of the extra term $\Omega_{n,0}$. The other observational test methods like CMB and the age of oldest objects in the Universe are also used. We use as well the Akaike informative criterion to select a model which best fits data and we concluded that the bouncing term should be ruled out by Occam's razor, which makes the big-bang scenario more favorable than the bouncing scenario.

DOI: 10.1103/PhysRevD.72.063504 PACS numbers: 98.80.Bp, 11.25.−w, 98.80.Cq

I. INTRODUCTION

We are living in an age of high precision cosmology which offers the possibility of testing exotic physics, which is obvious for the early Universe [1]. In this context the most important are BBN constraints because the present Universe opens only small windows on the exotic physics. The main aim of this paper is to discuss whether the initial singularity can be checked against the astronomical observations. The question of singularity cannot be answered directly, therefore we use two prototype models based on the classical and quantum gravity theory. The first is the ΛCDM which is a concordance model describing the evolution of the Universe from the initial singularity (the big bang) driven by the cold dark matter and the cosmological constant (dark energy). The second is a bouncing model which appears in the context of quantum cosmology and characterized by the lack of initial singularity. During its evolution, the expansion phase is proceeded by the contraction phase at the bounce where the scale factor assumes the minimum nonzero value.

We use some tests to discriminate between these two alternative models. One of the most important tests applies the SNIa data to fit the cosmological models. Recent measurements of type Ia supernovae observations suggest that the universe is presently accelerating [2,3]. A dark energy component has usually been proposed as a source of acceleration mechanism [4]. Many theoretical propositions have been suggested about these components. However, the different effects arising from quantum fluctuation, spinning fluid, etc. can also mimic dynamically the role the dark energy which drives acceleration through an additional term in the Friedmann equation [5–14]. Some of them give rise to the bounce. In many cases they prevailed in the very early epoch but are very small in the present epoch. Therefore it is very difficult to detect the existence of this component in the present and those of the relatively close past (after CMB) observations of SNIa.

In the present work we investigate observational constraints on the evolutionary scenario of the standard bouncing cosmological models defined as a class of models for

*Electronic address: uoszydlo@cyf-kr.edu.pl

which the Hubble function H and the scale factor a are related by the formula

$$H^2 = H_0^2(\Omega_{m,0}x^{-m} - \Omega_{n,0}x^{-n}), \tag{1}$$

where $n > m > 0$ and $x = \frac{a}{a_0}$, where the index zero denotes the quantities evaluated in the present epoch, the parameter $\Omega_{n,0}$ is called the bouncing term, and the density parameters satisfy the constraint relation

$$\Omega_{m,0} - \Omega_{n,0} = 1.$$

While we focus mainly on the constraints coming from SN Ia data and WMAP observations, the complementary constraints coming from BBN and the age [15] of the oldest high-redshift objects are also considered. We use the maximum likelihood method to estimate the model parameters m, n, and $\Omega_{n,0}$. Similarly we analyze the models with the additional parameter—the cosmological constant. It is called the generalized bouncing model.

The proposition of the bounce-type evolution of the early universe seems to be very attractive not only from the point of view of the quantum description of the early Universe because the expansion of the universe is accelerated automatically due to the presence of the bouncing term.

The standard bouncing scenario predicts the acceleration around the bounce with a transition to the deceleration epoch. The cosmological constant brings this deceleration epoch to the end and a new acceleration epoch begins.

Therefore, these models can be proposed as the models of our Universe, because they include the epoch of acceleration. However, we show that the influence of the bouncing term is insignificant in the present epoch. Therefore, the data from the present epoch, such as the SNIa data, do not have power to consider the model with the bouncing term statistically significant. So the ΛCDM model with the big-bang scenario is strongly favored by data over the model with the bounce.

By the application of standard Akaike criterion of the model selection, we can choose the ΛCDM model over the generalized bouncing model. We conclude that the data fail to support the existence of the bouncing term. The bouncing term in the present epoch is insignificant and it is not possible to detect its influence by the use of the latest SNIa data.

This fact justifies certain scepticism about the existence of the SNIa window on exotic physics in the current epoch. However, we cannot rule out other models by testing them against the current data. It is also possible to investigate the differences in the predictions of these models for some earlier epoch.

For example, the BBN epoch is a well tested area of cosmology. From this analysis we gather that the extra term $\Omega_{n,0}x^{-n}$ causing the bounce should be constrained to be sufficiently small during nucleosynthesis.

The organization of the text is the following. In Sec. II the evolutionary scenario of bounce Friedmann-Robertson-Walker (FRW) cosmologies is investigated by the use of dynamic system methods. We show that they are structurally unstable due to the presence of centers in the phase portraits. In Sec. III we discuss the constraints from SNIa data on the standard bouncing models. In Sec. IV we extend the bouncing models by introducing the cosmological constant and then we study how these models fit the current supernovae and WMAP data. In Sec. V we formulate conclusions.

II. THE BOUNCING MODELS: BASIC EQUATIONS

The idea of bounce in FRW cosmologies appeared in Tolman's monograph devoted to cosmology [16]. This idea was strictly connected with oscillating models [17–19]. At present, oscillating models play an important role in the brane cosmology [20,21]. The FRW universe undergoing a bounce instead of the big bang is also an appealing idea in the context of quantum cosmology [22]. The attractiveness of bouncing models comes from the fact that they have no horizon problem and they explain the quantum origin of structures in the Universe [23–25]. Molina-Paris and Visser and later Tippett [26,27] characterized the bouncing models by the minimal condition under which the present universe arises from a bounce from the previous collapse phase (the Tolman wormhole is a different name for denoting such a type of evolution). The violation of a strong energy condition (SEC) is in general a necessary (but not sufficient) condition for bounce to appear. For closed models it is a sufficient condition and none of the other energy conditions need to be violated [like null energy condition (NEC), $\rho + p \geq 0$; week energy condition (WEC), $\rho \geq 0$ and $\rho + p \geq 0$; dominant energy condition (DEC), $\rho \geq 0$ and $\rho \pm p \geq 0$ energy conditions can be satisfied].

We can find necessary and sufficient conditions for an evolutional path with a bounce by analyzing dynamics on the phase plane $(a, \dot{a})$, where a is the scale factor and the dot denotes differentiation with respect to cosmological time. We understand the bounce as in [26,27], namely, there must be some moment, say $t = t_{\text{bounce}}$, in evolution of the universe at which the size of the universe has a minimum, $\dot{a}_{\text{bounce}} = 0$ and $\ddot{a} \geq 0$. This weak inequality $\ddot{a} \geq 0$ is enough for giving domains in the phase space occupied by trajectories with the bounce. Let us consider the dynamics of the FRW cosmological models filled by perfect fluid with energy density ρ and pressure p parametrized by the equation of state in the general form

$$p = w(a)\rho. \tag{2}$$

The basic dynamical system constitutes two equations:

$$\frac{\ddot{a}}{a} = -\frac{1}{6}(\rho + 3p), \tag{3}$$

$$\dot{\rho} = -3H(\rho + p). \tag{4}$$

Equation (3) is the Rauchadhuri equation while Eq. (4) is the conservation condition. If the equation of state is postulated in the form (2), then from (4) we obtain

$$\rho = \rho(a) = \rho_0 a^{-3} \exp\left(-3 \int^a \frac{w(a)}{a} da\right). \tag{5}$$

It is interesting that dynamics of the model under consideration can be represented in the analogous form to the Newtonian equation of motion

$$\ddot{a} = -\frac{\partial V}{\partial a}, \tag{6}$$

where $V = -\frac{\rho a^2}{6}$ plays the role of a potential function for the FRW system. Therefore different cosmological models are in a unique way characterized by the potential function $V = V(a)$ and we can write down the Hamiltonian for the fictitious particle-universe moving in the one-dimensional potential as

$$\mathcal{H} = \frac{p_a^2}{2} + V(a), \qquad p_a = \dot{a}. \tag{7}$$

It is useful to represent Eq. (6) in the form of dynamical system,

$$\dot{x} = y, \qquad \dot{y} = -\frac{\partial V}{\partial x}, \tag{8}$$

where we denote $x = a$, $y = \dot{a}$, and system (8) has the first integral in the form

$$\frac{y^2}{2} + V(x) = -\frac{k}{2}, \tag{9}$$

where k is the curvature index.

The critical points of the system (8) if they exist are $y_0 = 0$, $(\frac{\partial V}{\partial x})_{x_0} = 0$; i.e. they are always static critical points located on the x-axis. The form of the first integral (9) defines the algebraic curves in the phase plane $(a, \dot{a})$ on which lie solutions of the system. These solutions are in two types: regular is represented by trajectories or singular is represented by singular solutions for which the right-hand side of (8) are null [or $V(x_0) = -\frac{k}{2}$ for nonflat models]. Note that the bouncing points are intersection points of trajectories situated in the region of the configuration space in which $\frac{\partial V}{\partial a} \leq 0$, i.e. $V(a)$ is a decreasing function of a or has extrema. It is well known that the systems in the form (8) have only critical points of two admissible types: centers if $[(d^2V)/(dx^2)]_{x_0} > 0$ or saddles in the opposite case if $[(d^2V)/(dx^2)]_{x_0} < 0$. Therefore all trajectories with bounce intersect an x-axis and then they are situated on the right side from the critical point at which $\dot{a} = 0$ and $\ddot{a} \geq 0$. The critical points are represented by points as well as by separatrices of the saddle point. In others words, bouncing trajectories are represented by such trajectories in the phase plane which are passing through the x-axis in such a direction that they always belong to the accelerating region (in the neighborhood of bounce). Of course it is only possible if the SEC is violated.

Let us consider some prototype of bouncing models given by the Friedmann first integral in the form

$$H^2 = \frac{A}{a^m} - \frac{B}{a^n}, \tag{10}$$

where A, B are positive constants and $n > m$, $H = (\ln a)^{\cdot}$ is the Hubble function, and a dot denotes differentiation with respect to cosmological time t.

It is convenient to rewrite (10) to the new form

$$H^2 = H_0^2(\Omega_{m,0} x^{-m} - \Omega_{n,0} x^{-n}), \tag{11}$$

where $\Omega_{m,0}$, $\Omega_{n,0}$ are density parameters for noninteracting fluids which give some contributions to the right-hand side of Eq. (10). We define density parameters $\Omega_{m,0} = (3Aa^{-m})/(3H_0^2)$, $\Omega_{n,0} = (3Ba^{-n})/(3H_0^2)$, where an index "0" means that corresponding quantities are evaluated at the present epoch, $x = \frac{a}{a_0}$ is the scale factor expressed in the units of its present value a_0.

After differentiation of both sides of (11) with respect to the reparametrized time variable $\tau : t \rightarrow \tau$, $|H_0|dt = d\tau$, we obtain

$$\frac{\ddot{x}}{x} = \frac{1}{2}(\Omega_{m,0}(2 - m)x^{-m} + \Omega_{n,0}(n - 2)x^{-n}). \tag{12}$$

If we consider the generalization of the bouncing models with the cosmological constant, then in both equations (11) and (12) the parameter $\Omega_{\Lambda,0}$ should be added to their right-hand sides.

Note that the bouncing models can be treated as the standard FRW models with two noninteracting fluids with energy density and pressure in the form

$$\rho = \rho_m + \rho_n = 3H_0^2\Omega_{m,0}x^{-m} - 3H_0^2\Omega_{n,0}x^{-n}$$

$$p = \left(-1 + \frac{m}{3}\right)\rho_m + \left(-1 + \frac{n}{3}\right)\rho_n \qquad \rho_m > 0, \rho_n < 0.$$

The curvature term as well as the cosmological constant term can be obtained in an analogous way by putting $m = 2$ or $m = 0$, respectively.

If we postulate that the present universe is accelerating, i.e. $\ddot{x} > 0$ at $x = 1$, then in the general case with the cosmological constant we obtain the following condition:

$$\Omega_{m,0}(2 - m) + \Omega_{n,0}(n - 2) + 2\Omega_{\Lambda,0} > 0. \tag{13}$$

Because relation (13) is valid any time, the substitution $H = H_0$ and $x = 1$ to (13) gives the constraint

$$\Omega_{m,0} - \Omega_{n,0} + \Omega_{\Lambda,0} = 1. \tag{14}$$

Let us now concentrate on the standard bouncing models (SB) without the cosmological term. Then from (13) including constraints (14) we obtain the sufficient condition for acceleration at present:

$$\Omega_{m,0}(n-m) > 2-n, \tag{15}$$

where for the case of $n=2$, $k=1$ $\Omega_{m,0}>0$ is only required for the present acceleration.

If only $\Omega_{n,0}$ is larger than $\Omega_{m,0}$, the bouncing universe is presently accelerating for any parameters m, n. It is worth mentioning that condition (15) is minimal qualitative information about acceleration and the rate of this acceleration is required for explanation of SNIa data.

From the definition (11), one can obtain the domain admissible for motion of the bouncing models:

$$D = \left\{x: x \geq x_{\mathrm{b}} \text{ where } x_{\mathrm{b}} = \left(\frac{\Omega_{n,0}}{\Omega_{m,0}}\right)^{1/(n-m)}\right\}. \tag{16}$$

From (11) the potential function $V(x)$ in the particlelike description can be determined:

$$V(x) = -\frac{\rho_{\mathrm{eff}}x^2}{6H_0^2} = -\frac{1}{2}\Omega_{\mathrm{eff}}(x)x^2, \tag{17}$$

where effective density parameter $\Omega_{\mathrm{eff}} = \Omega_{m,0}x^{-m} - \Omega_{n,0}x^{-n}$. The acceleration region in the phase plane can be determined in terms of potential function, namely, if

$$\frac{dV}{da} < 0, \tag{18}$$

then universe is accelerating.

From (17) we obtain the result that at the bounce moment

$$\ddot{x} = -\left(\frac{dV}{dx}\right)_{x_b} = \frac{1}{2}\Omega_{m,0}\left(\frac{\Omega_{m,0}}{\Omega_{n,0}}\right)^{m/(m-n)}(n-m), \tag{19}$$

which indicates that bouncing models defined by Eq. (11) at the bounce are in the accelerating phase for any ranges of model parameter $m, n, \Omega_{m,0}, \Omega_{n,0}$. Because a_b is larger than $a_0 : (\frac{dV}{da})_{a_0} = 0$, the bouncing universe stays still in the accelerating region.

From Eq. (19) we obtain that the universe starts to accelerate at the point $x = x_0$ such that

$$x_0 = \left(\frac{\Omega_{m,0}(m-2)}{\Omega_{n,0}(n-2)}\right)^{1/(m-n)}, \tag{20}$$

where a positive value of $(m-2)(n-2)$ is required. Note that in any case

$$x_0 < x_b, \tag{21}$$

i.e., the start of acceleration precedes the bounce. The value of x_0 determines the location of the critical point of the dynamical system $\dot{x} = y, \dot{y} = -\frac{\partial V}{\partial x}$ on the x-axis. The sign of the second derivative of potential function determines the type of critical points (center or saddle) because the eigenvalues of the linearization matrix of the system satisfy the characteristic equation,

$$\lambda^2 + \left(\frac{\partial^2 V}{\partial x^2}\right)(x_0) = 0. \tag{22}$$

From (17) we obtain

$$\left(\frac{\partial^2 V}{\partial x^2}\right)(x_0) = -\frac{1}{2}\Omega_{n,0}x_0^{-n}[(2-m)(1-m) - (2-n)(1-n)]. \tag{23}$$

Therefore if (m, n) belong to the interval $(3/2, \infty)$ then we have centers, while if (m, n) belong to the interval $(-\infty, 3/2)$ we obtain saddles.

Let us concentrate, for example, on the case of $m = 3$ (dust matter). Then

$$\left(\frac{\partial^2 V}{\partial x^2}\right)(x_0) = \frac{1}{2}\Omega_{n,0}x_0^{-n}n(n-3). \tag{24}$$

Hence, if $n > 3$ we obtain $(\frac{\partial^2 V}{\partial x^2})(x_0)$ positive which corresponds to the centers in the phase plane. The presence of centers on the phase portraits means that all bouncing models are oscillating. Let us note, however, that the corresponding systems are structurally unstable because of the presence of nonhyperbolic critical points on the phase portraits. Physically it means that the small perturbation of right-hand sides of the system under consideration disturbs a qualitative structure of the orbits (i.e. a phase portrait). In Figs. 1 and 2 the phase portraits and diagrams of the potential function are presented for the standard and generalized bouncing models. Figure 1 describes all special cases listed in Table I. The classically forbidden region for $a < a_0$ is shaded. The evolution of the model is represented in the configuration space by a Hamiltonian level,

$$\mathcal{H} = E = \frac{1}{2}\Omega_{k,0}.$$

The trajectory of the flat model separates the regions occupied by both closed and open models. The decreasing of the potential function with respect to the scale factor determines the domain of phase space occupied by accelerating trajectories. The bounce is the intersection point of trajectory with the axis a. Note that around the bounce we have acceleration. On the phase plane of Hamiltonian dynamical systems, only centers and saddle points are admissible. The centers are structurally unstable while saddles are structurally stable. Because the center appears in the phase portraits of standard and generalized bouncing models, both models are structurally unstable. The critical points represent the static universes. The generalized bouncing model has two disjoint acceleration regions. The first is due to the bouncing term while the second is forced by the cosmological constant term.

Full knowledge of the dynamics required its analysis at infinity, i.e. at the circle at infinity $x^2 + y^2 = \infty$. The standard procedure is to use projective maps on the plane and then analyze the system in a standard way. One can find the critical points at infinity as an intersection of the trajectory of a flat model with the circle at infinity,

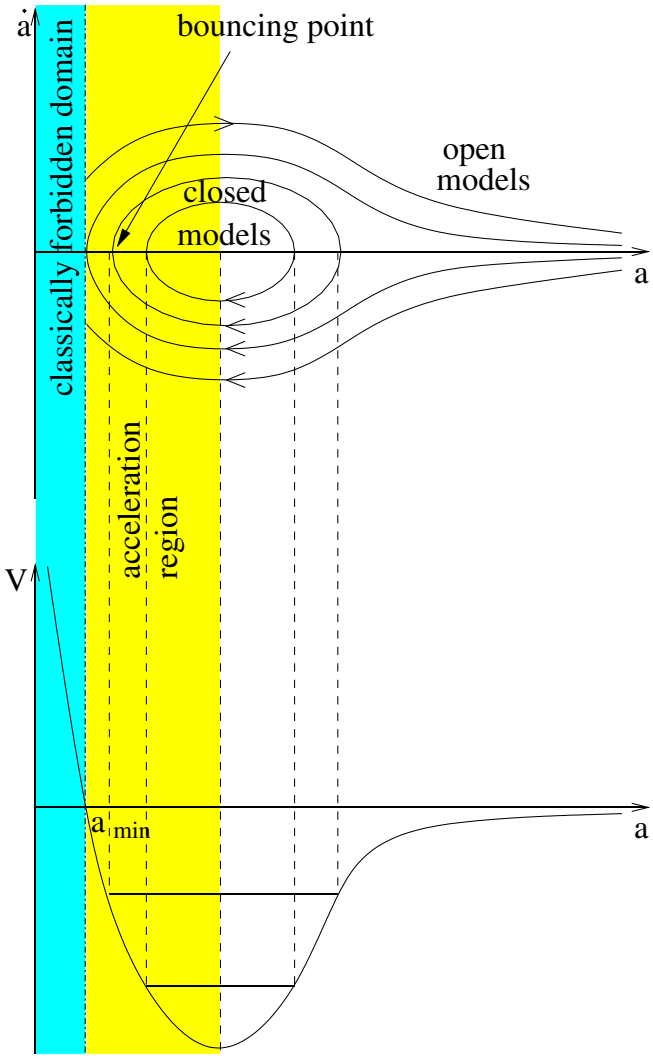

FIG. 1 (color online). The phase portrait and the diagram of the potential function for BM model (all cases from Table I). The minimum of the potential function corresponds to a center on the phase plane. The acceleration region is located on the right from the $a_{\min}$.

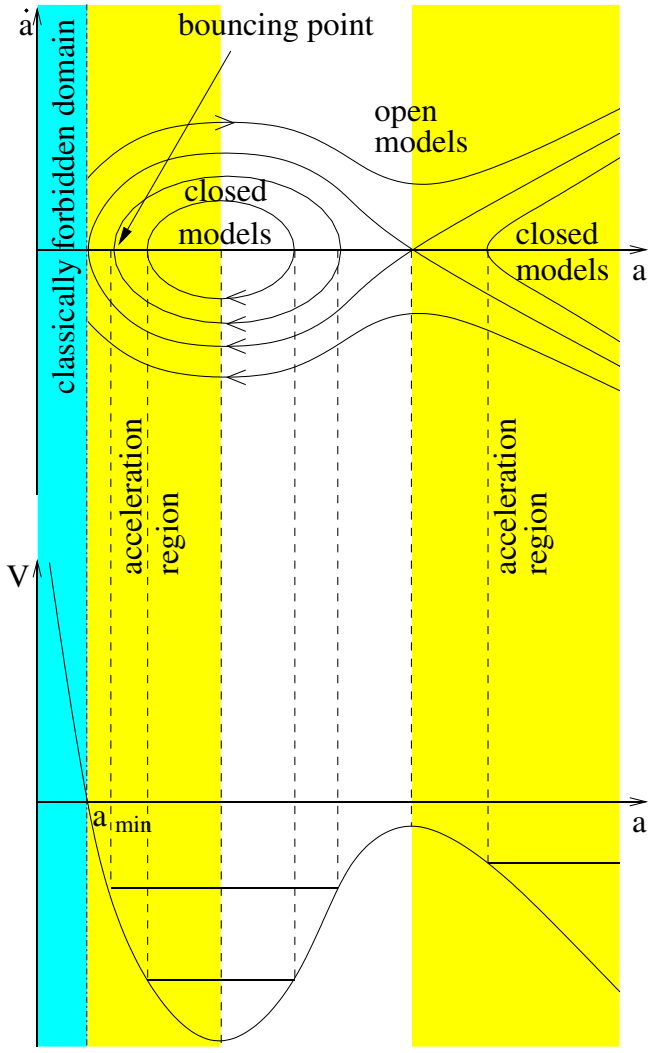

FIG. 2 (color online). The phase portrait and the diagram of the potential function for the ΛBCDM model. The minimum (maximum) of the potential function corresponds to a center (saddle) on the phase plane. The system is structurally unstable because of the presence of a nonhyperbolic critical point (a center).

i.e. $\{(x, y) : \Omega_{k,0} = 0\}$ and $\{z = 1/x, u = y/x,$ and $x = \infty, v = 1/y, w = x/y, y = \infty\}$—the trajectory of the flat model $\frac{y^2}{2} = -V(x)$ with a circle at infinity.

Some special cases of the bouncing systems are shown in Table I. Because we are dealing with autonomous dynamical systems, their phase portrait is always given modulo diffeomorphism or equivalent modulo any time reparametrization follows the rule $\tau \rightarrow \eta : d\tau = f(x)d\eta$, where $f(x)$ is diffeomorphism, and x is the point which belongs to phase plane.

For analysis of bouncing models in terms of dynamical systems, it is useful to reparametrized the original time variable in order to obtain nondegenerate critical points at infinity. Then we obtain $\frac{d\tau}{x^{\beta/2}}$ and $\frac{y^2}{2} = \frac{1}{2}(\Omega_{m,0}x^{2-m+\beta} - \Omega_{n,0}x^{2-n+\beta})$ is now representing the trajectory of the flat model; β should be chosen in the suitable way to regularize critical points. Let $\beta = n - 2$, then as x goes to infinity y also goes to infinity. Only the sign of the parameter m (if $m < 0$) decides whether the future of the system is the type of a big-rip singularity. If $m = 0$, then the case of the cosmological constant can be recovered.

It is convenient to regularize the system by multiplication of both sides of the system x^3 in the first case and x^4 in the second one, respectively. It is equivalent to reparametrized time variable following the rule $\tau \rightarrow \eta : \frac{d\tau}{x^\beta} = d\eta$, where $\beta = 3$ and (5) for the system from Table I. For both systems from the table, we have an additional term in the generalized FRW equation. In the first case the effects of global rotation produce a contribution corresponding to the negative energy scaling like radiation. The same contribu-

TABLE I. Some special cases of bouncing models.

Model	Dynamical equations (first integral)
FRW model dust filled	$\dot{x} = yx^3$
universe with global rotation [14]	$\dot{y} = \frac{1}{2}(-\Omega_{m,0}x^{-2} + 2\lvert\Omega_{\omega,0}\rvert x^{-3})x^3$
or brane models with dark radiation [28]	$\frac{y^2}{2} = \frac{1}{2}(-\Omega_{m,0}x^{-1} - \lvert\Omega_{\omega,0}\rvert x^{-2} + \Omega_{k,0})x^6$
FRW dust filled	$\dot{x} = yx^5$
universe with spinning fluid [29]	$\dot{y} = \frac{1}{2}(-\Omega_{m,0}x^{-2} + 4\lvert\Omega_{s,0}\rvert x^{-5})x^5$
or a class of MAG models [30]	$\frac{y^2}{2} = \frac{1}{2}(-\Omega_{m,0}x^{-1} - \lvert\Omega_{s,0}\rvert x^{-4} + \Omega_{k,0})x^{10}$
Stephani models	$\dot{x} = y$
filled by perfect fluid	$\dot{y} = \frac{1}{2}(-\Omega_{\gamma,0}(1+3\gamma)x^{-2-3\gamma} + \delta\Omega_{k,0}x^{\delta-1})$
$p = \gamma\rho$ [13]	$\frac{y^2}{2} = \frac{1}{2}(\Omega_{\gamma,0}x^{-1-3\gamma} + \Omega_{k,0}x^{\delta})$

tion appears in the brane models on the charged brane. It is known as the dark radiation [10]. Please note that an analogous term appeared if we include the Casimir effect coming, for example, from quantum effects of massless scalar fields [22,31,32]. In the second case (Table I), it is the model with spinning dust fluid. It can also be recovered as a class of MAG models [7,30].

In both cases, we can find the center at finite domain and periodic orbits. At infinity we have unstable and stable nodes at $x = +\infty, y = \mp\infty$. The trajectory of the flat model separates the regions occupied by closed and open models. All models have bounce but some of them are oscillating models without the initial and final singularities. For our future investigations of observational constraints on bouncing models, it is convenient to derive crucial formulas for $H(z)$ where z is redshift $z : 1 + z = x^{-1}$. We obtain from (10) that $H^2 = H_0^2[\Omega_{m,0}(1+z)^m - \Omega_{n,0}(1+z)^n]$. It is useful to represent it in the corresponding bouncing parameters.

For this aim we find x_b corresponding to the bounce and value of redshift which identify this moment during the evolution: $x_b = (\frac{\Omega_{n,0}}{\Omega_{m,0}})^{1/(n-m)}$, $z_b = -1 + (\frac{\Omega_{m,0}}{\Omega_{n,0}})^{1/(n-m)}$. Finally, we obtain independent model parameters characterizing its role in evolution (modulo present value of H_0), namely,

$$H = H_0\sqrt{\frac{(1+z_b)^{n-m}}{(1+z_b)^{n-m}-1}}(1+z)^{m/2}\sqrt{1+\left(\frac{z+1}{z_b+1}\right)^{n-m}}. \tag{25}$$

If $\Omega_{m,0}$ is fixed, for example, from independent galaxy observations, then the evolutionary scenario is parametrized by single n parameter

$$H = H_0\sqrt{\Omega_{3,0}}(1+z)^{3/2}\sqrt{1+\left(1-\frac{1}{\Omega_{3,0}}\right)(1+z)^n}, \tag{26}$$

where we put $\Omega_{m,0} = \Omega_{3,0}$, i.e. dust filled universe.

In the case of generalized bouncing models, the potential function takes the following form:

$$V(x) = \frac{1}{2}\Omega_{n,0}x^{2-n} - \frac{1}{2}\Omega_{m,0}x^{2-m} - \frac{1}{2}\Omega_{\Lambda,0}x^2.$$

It means that if only $n, m > 0$ then we obtain the de Sitter solution as a global attractor in the future. In the opposite case if $m > 0$ the big-rip singularities are the generic future of the model. Note that in the class of generalized bouncing models only trajectories around point $(x_0, 0)$ represent oscillating models without a singularity and there is an admissibly large class of closed, open, and flat models which evolve to infinity.

It is interesting that the characteristic bounce can be defined in terms of geometry of potential function only. By bouncing cosmology we can understand all cosmological models for which the potential function has at some point a minimum.

III. BOUNCING MODEL AND DISTANT SUPERNOVAE OBSERVATIONS

In this section we confront the bouncing cosmological models with observations of distant SNIa. These observations in the framework of the FRW model indicate that present acceleration of our Universe is due to an unknown form of matter with negative pressure called dark energy [3]. Apart from the cosmological constant there are also other candidates for dark energy which were tested from SNIa observations [33–35]. We use the SNIa data to test the acceleration in the bouncing models. Moreover, these models are attractive because they have no horizon and initial singularity, and they yield an explanation of structures which originated in the quantum epoch [22].

We consider the flat FRW model since there is very strong evidence that the Universe is flat in the light of recent WMAP data [36]. We confront the two ''bouncing'' models (with and without extra Λ fluid) with SNIa data. For this purpose we calculate the luminosity distance in a standard way,

$$d_L(z) = (1+z)\int_0^z \frac{d\bar{z}}{H(\bar{z})}. \tag{27}$$

To proceed with fitting models to SNIa data, we need the magnitude-redshift relation

$$m(z, \mathcal{M}, \Omega_{m,0}, \Omega_{\Lambda,0}, n, m) - M = \mathcal{M} + 5\log_{10} D_L(z, \Omega_{m,0}, \Omega_{\Lambda,0}, m, n), \tag{28}$$

where M being the absolute magnitude of SNIa and

$$D_L(z, \Omega_{m,0}, \Omega_{\Lambda,0}, m, n) = H_0 d_L(z, H_0, \Omega_{m,0}, \Omega_{\Lambda,0}, m, n) \tag{29}$$

is the luminosity distance with H_0 factored out, so that marginalization over the parameter $\mathcal{M}$

$$\mathcal{M} = -5\log_{10} H_0 + 25 \tag{30}$$

reads actually marginalization over H_0.

The parameter $\mathcal{M}$ is actually determined from the low-redshift part of the Hubble diagram which should be linear in all realistic cosmologies. It leads to the value of $H_0 \simeq 65$ km/s Mpc [2,3,37], i.e., $\mathcal{M} \simeq 15.955$. In further analysis we estimate the models with this value of $\mathcal{M}$ and without any prior assumption on H_0.

Then we can obtain the best-fit model minimizing the function χ^2,

$$\chi^2 = \sum_i \frac{(\mu_i^{\text{theor}} - \mu_i^{\text{obs}})^2}{\sigma_i^2}, \tag{31}$$

where the sum is over the SNIa sample and σ_i denote the (full) statistical error of magnitude determination and $\mu_i = m_i - M_i$.

Because the best-fit values alone are not sufficient, the statistical analysis is supplemented with the confidence levels for the parameters. We performed the estimation of model parameters using the minimization procedure, based on the maximum likelihood method. We assume that supernovae measurements came with uncorrelated Gaussian errors and the likelihood function $\mathcal{L}$ could be determined from the chi-square statistic $\mathcal{L} \propto \exp(-\chi^2/2)$ [2].

The first published large samples of SNIa appeared at the end of the 1990s [2,3]. Later other data sets have been made either by correcting errors or by adding new supernovae. The latest compilation of SNIa was prepared by Riess *et al.* [37] and became *de facto* a standard data set. It should be noted that this compilation encloses the largest number of high-redshift $z > 1.25$ objects in comparison to older compilations. From this compilation we take the "Silver" sample which contains all 186 SNIa, and the restricted "Gold" sample of 157 SNIa (with higher quality of the spectroscopic and photometric records).

In order to test a cosmological model, we calculate the best fit with minimum χ^2 as well as estimate the model parameters using the maximum likelihood method [2]. For both statistical methods we take the parameters m and n in the interval $[0, 10]$, $n > m$. We test separately the models with and without the cosmological constant term. We also assume priors about $\Omega_{\text{m},0}$ and we estimate it or take $\Omega_{\text{m},0} = 0.3$ (baryonic plus dark matter in galactic halos) [38].

TABLE II. Results of the statistical analysis of the bouncing model without dust (BM) and bouncing cold dark matter model (BCDM) obtained for SNIa data from the best fit with minimum χ^2 (denoted as BF) and from the likelihood method (denoted as L). The case of a fixed value of the parameter $\mathcal{M}$ is denoted as F. If in the BF method we obtain $\Omega_{\text{n},0} = 0$ then n could be taken as arbitrary (marked as A).

Model	$\Omega_{m,0}$	m	$\Omega_{n,0}$	n	$\mathcal{M}$	χ^2	Method
BM model	1.00	1.4	0.00	A	15.975	181.6	BF
	1.00	1.5	0.00	1.7	15.975	···	L
	1.54	1.4	0.54	1.5	F15.955	182.3	BF
	1.00	1.4	0.00	1.6	F15.955	···	L
BCDM model	1.86	···	0.86	3.7	16.085	217.4	BF
(dust matter $m = 3$)	1.86	···	0.86	3.7	16.095	···	L
	1.86	···	0.86	3.7	F15.955	273.7	BF
	1.86	···	0.86	3.7	F15.955	···	L

The results of two fitting procedures performed on the Gold sample for the cosmological bouncing models with different prior assumptions are presented in Tables II and III. These tables refer both to the χ^2 (best fit) and results from marginalized probability of density functions.

At first we analyzed bouncing model without any priors for the m parameter (BM). We obtain the value $\chi^2 = 181.6$ which means that this model is acceptable on the 2σ level with a degree of freedom df $= 153$. However, the estimated value of $m = 1.4$ in the model is unrealistic because the dust matter is present in the universe ($m = 3$). With the prior $m = 3$ we obtain $\chi^2 = 217.4$ with the value of the parameter $n = 3.7$. For the more realistic model with $m = 3$ and $n = 4$ (because of the presence of radiation matter in

TABLE III. The results of statistical analysis of BCDM models ($m = 3$) obtained for SNIa data from the best fit with minimum χ^2 (denoted as BF) and from the likelihood method (denoted as L). The case of a fixed value of $\mathcal{M}$ is denoted as F.

Model	$\Omega_{m,0}$	$\Omega_{n,0}$	$\mathcal{M}$	χ^2	Method
BCDM model	1.50	0.50	16.105	226.6	BF
with $n = 4$	1.50	0.50	16.095	···	L
	1.50	0.50	F15.955	296.4	BF
	1.50	0.50	F15.955	···	L
BCDM model	1.03	0.03	16.175	291.2	BF
with $n = 6$	1.03	0.03	16.175	···	L
	1.03	0.03	F15.955	443.4	BF
	1.03	0.03	F15.955	···	L

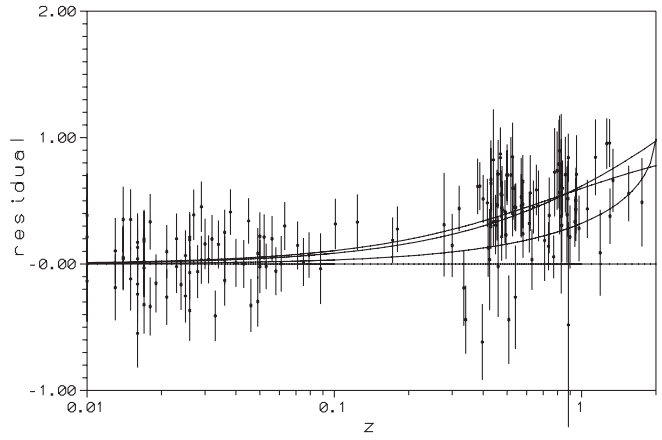

FIG. 3. Residuals (in mag) between the Einstein-de Sitter model and the Einstein-de Sitter itself (zero line), the ΛCDM flat model (upper curve), the best-fitted BM model (upper-middle curve), and the best-fitted BCDM model with $m = 3$ (lower-middle curve) (with assumed $\mathcal{M} = 15.955$).

the Universe) (Table III), we obtain $\chi^2 = 226.6$. While the bouncing model with dust (BCDM) is better fitted than the Einstein-de Sitter model it is rejected at least on the 4σ level. With priors $\mathcal{M} \simeq 15.955$ the model is rejected on the 8σ level.

In Fig. 3 we present residuals plots of the m-z relation for considered models with respect to the Einstein-de Sitter (CDM) model. Apart from the CDM model (the zero line), the three models ΛCDM, BM, and BCDM are shown. The diagrams for bouncing models intersect the ΛCDM diagram in such a way that the supernovae on intermediate distances are brighter than expected in the ΛCDM model, while very high-redshift supernovae should be fainter than they are expected in the ΛCDM model. Note that this effects are more stronger for the BCDM model than for the BM model.

TABLE IV. Results of the statistical analysis of the extended bouncing models ($m = 3$), obtained for SNIa data from the best fit with minimum χ^2 (denoted as BF) and from the likelihood method (denoted as L). The case of a fixed value of parameter $\Omega_{m,0}$ is denoted as F. If in BF method we obtain $\Omega_{\mathrm{n},0} = 0$ then n could be taken as arbitrary (marked as A).

Model	$\Omega_{m,0}$	$\Omega_{n,0}$	n	$\Omega_{\Lambda,0}$	$\mathcal{M}$	χ^2	Method
ΛBCDM model	0.31	0.00	A	0.69	15.955	175.9	BF
	0.34	0.00	3.0	0.67	15.965	···	L
	F0.30	0.00	A	0.70	15.955	175.9	BF
	F0.30	0.00	3.0	0.70	15.945	···	L
ΛBCDM model	0.31	0.00	A	0.69	···	175.9	BF
with $\mathcal{M} = 15.955$	0.31	0.00	3.0	0.68	···	···	L
	F0.30	0.00	A	0.70	···	175.9	BF
	F0.30	0.00	3.0	0.70	···	···	L

TABLE V. Results of comparison of ΛCDM model with the extended bouncing models ($m = 3$) with fixed values $n = 4$ and $n = 6$. The result of statistical analysis for SNIa data from the best fit with minimum χ^2 (denoted as BF) and from the likelihood method (denoted as L). The case of a fixed value of $\Omega_{m,0}$ is denoted as F.

Model	$\Omega_{m,0}$	$\Omega_{n,0}$	$\Omega_{\Lambda,0}$	$\mathcal{M}$	χ^2	Method
ΛCDM model	0.31	···	0.69	15.955	175.9	BF
	0.34	···	0.67	15.965	···	L
	F0.30	···	0.70	15.955	175.9	BF
	F0.30	···	0.70	15.945	···	L
ΛBCDM model	0.31	0.00	0.69	15.955	175.9	BF
with $n = 4$	0.37	0.00	0.65	15.965	···	L
	F0.30	0.00	0.70	15.955	175.9	BF
	F0.30	0.00	0.70	15.945	···	L
ΛBCDM model	0.31	0.00	0.69	15.955	175.9	BF
with $n = 6$	0.34	0.00	0.66	15.965	···	L
	F0.30	0.00	0.70	15.955	175.9	BF
	F0.30	0.00	0.70	15.945	···	L

Similarly, we analyze the bouncing models with the additional parameter—the cosmological constant. We fixed a value of $m = 3$ (dust matter) and it is called the extended bouncing model (ΛBCDM). This model with $\mathrm{df} = 153$ is statistically admissible on the 2σ level (Table IV), but we obtain $\Omega_{n,0} = 0$ (no bounce term) as a most probable value. This result is similar also for models with fixed values $n = 4$ and $n = 6$ (Table V), as well as independent from the assumption on $\Omega_{\mathrm{m},0}$. In this way ΛBCDM reduces to the ''classical'' ΛCDM model.

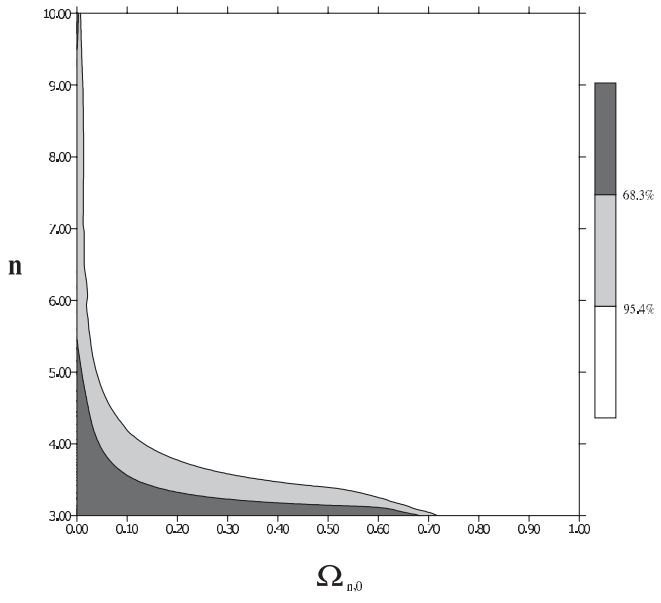

FIG. 4. For the extended bouncing model with $\mathcal{M} = 15.955$, there are shown the confidence levels on the plane $(\Omega_{n,0}, n)$ minimized over parameter $\Omega_{m,0}$.

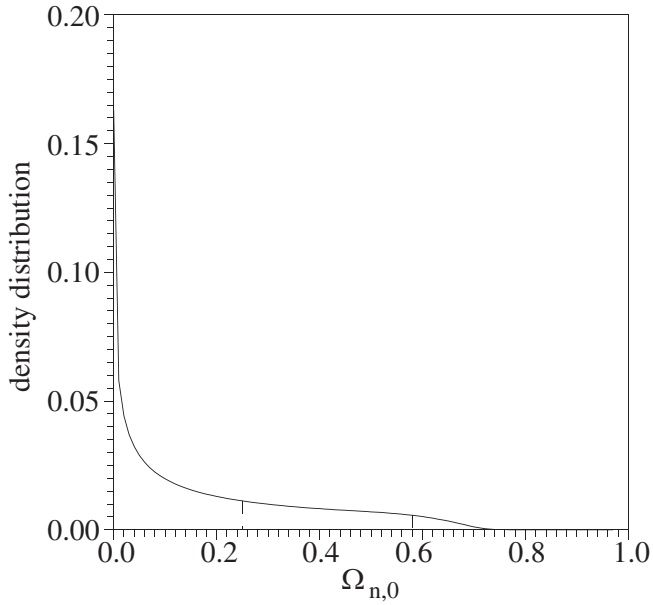

FIG. 5. Extended bouncing model with $\mathcal{M} = 15.955$. The density distribution for $\Omega_{n,0}$. Confidence level 68.3% and 95.4% are also marked on the figure.

The confidence levels in the $(\Omega_{n,0}, n)$ plane are presented in Fig. 4. In order to complete the picture, we have also derived one-dimensional probability distribution functions (PDF) for $\Omega_{n,0}$ (Fig. 5) and n (Fig. 6) obtained from the joint marginalization over remaining model parameters. The maximum value of such a PDF informs us about the most probable value of $\Omega_{n,0}$, supported by supernovae data within the extended bouncing dust model.

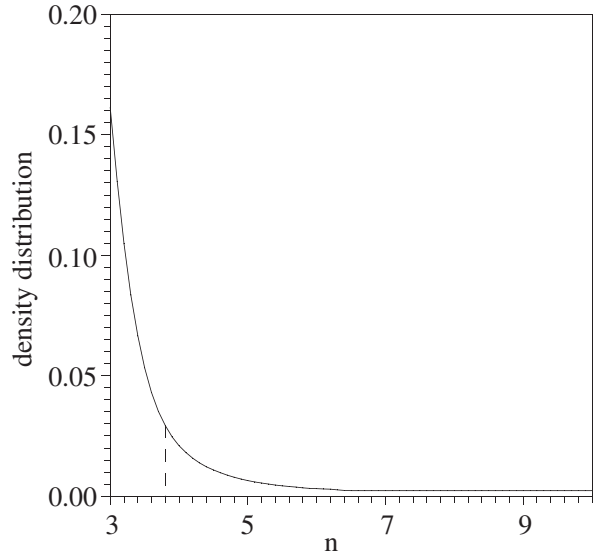

FIG. 6. Extended bouncing model with $\mathcal{M} = 15.955$. The density distribution for n. Confidence level 68.3% and 95.4% are also marked on the figure.

TABLE VI. The Akaike information criterion (AIC) for models under consideration: Einstein-de Sitter model (CDM), ΛCDM model (ΛCDM), bouncing model (BM), bouncing model with dust $m = 3$ (BCDM), and extended bouncing model with dust $m = 3$ (ΛBCDM).

Model	Number of parameters	AIC
CDM	1	325.5
ΛCDM	2	179.9
BM	4	189.6
BCDM	3	223.4
BCDM with $n = 4$	2	230.6
BCDM with $n = 6$	2	295.2
ΛBCDM	4	183.9
ΛBCDM with $n = 4$	3	181.9
ΛBCDM with $n = 6$	3	181.9

From the PDFs the most probable value of $\Omega_{n,0}$ is also equal to 0, however a nonzero value of $\Omega_{n,0}$ cannot be excluded. In this way, it is crucial to determine which combination of parameters gives the preferred fit to data. This is the statistical problem of model selection [39]. The problem is the elimination of parameters which play an insufficient role in improving the fit to data. The Akaike information criterion (AIC) plays an especially important role in this area [40]. This criterion is defined as

$$\mathrm{AIC} = -2\ln\mathcal{L} + 2k, \tag{32}$$

where $\mathcal{L}$ is the maximum likelihood and k is the number of the parameter of the model. The best model is the model which minimizes the AIC. The AIC for the models under consideration is presented in Table VI. It is clear that model which is minimizing AIC is ΛCDM. Therefore there is no reason to introduce a model with bouncing terms and such model should be ruled out by Occam's razor. Because the extended bouncing dust model is statistically admissible from SNIa data, it can be reconsidered only if the firm theoretical reason appears. Only this situation can justify consideration of the model with a small, but nonzero, bouncing term.

The existence of the oldest high-redshift extragalactic (OHReG) objects could be used as a test of the cosmological models (Table VII). The globular cluster analysis indicated that the age of the Universe is 13.4 Gyr [41]. We

TABLE VII. The age of extragalactic objects.

Number	Object	z	Age in Gys
1	Globular cluster	0	13–15
2	3C65 quasar	1.175	4.0
3	LBDS 53W069	1.43	4.0
4	LBDS 53W091	1.55	3.5

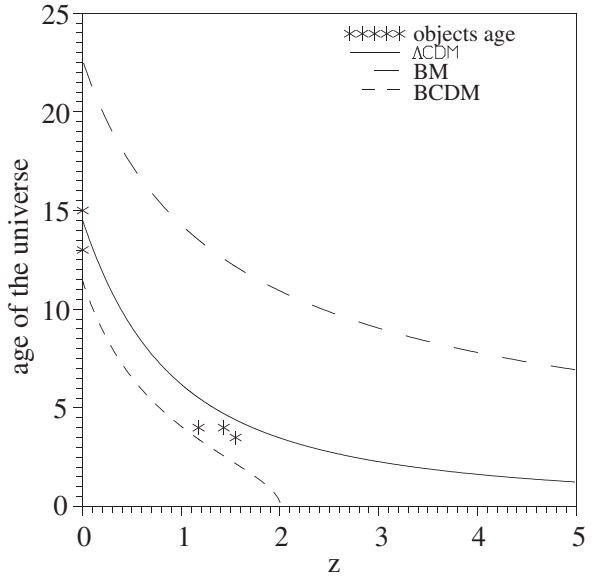

FIG. 7. The age of the Universe on particular z for three classes of models: ΛCDM (middle curve), bouncing model BM (upper curve), and bouncing model with dust matter BCDM (lower curve). We marked the age of 4 extragalactic objects by stars (Table VII).

demonstrate that the age of OHReG objects restricts the model parameter. As a criterion we believe that the age of the Universe in a given redshift should be bigger than, or at least equal to, the age of its oldest objects. With the assumption of $H_0 = 65$ km/s MPc, the age of the universe on particular z for three classes of models is calculated (Fig. 7). This test admits the ΛCDM model with $\Omega_{\mathrm{m},0} = 0.3$. In this model, the age of the Universe is 14.496 Gyr. The BM model seems to be allowed from this test, however, that model predicts a much longer age of the Universe (more than 20 Gyr) than ΛCDM. In turn, the BCDM model must be rejected because its age is 11.5 Gyr.

IV. CMB PEAKS IN THE EXTENDED BOUNCING MODEL

Acoustic oscillations in the primeval plasma during the last scattering give rise to the temperature map of cosmic microwave background (CMB). Peaks in the power spectrum correspond to maximum density of the wave. In the Legendre multipole space these peaks correspond to the angle subtended by the sound horizon at the last scattering. Further peaks answer to higher harmonics of the principal oscillations.

The locations of these peaks depend on the variations in the model parameters. Therefore, they can be used to constrain the parameters of cosmological models.

The acoustic scale ℓ_A which puts the locations of the peaks is defined as

$$\ell_A = \pi \frac{\int_0^{z_{\mathrm{dec}}} \frac{dz'}{H(z')}}{\int_{z_{\mathrm{dec}}}^{\infty} c_s \frac{dz'}{H(z')}}, \tag{33}$$

where

$$H(z) = H_0 \sqrt{\Omega_{\mathrm{m},0}(1+z)^3 + \Omega_{\mathrm{r},0}(1+z)^4 - \Omega_{n,0}(1+z)^n + \Omega_{\Lambda,0}} \tag{34}$$

and c_{s} is the speed of sound in the plasma given by

$$c_{\mathrm{s}}^2 \equiv \frac{dp_{\mathrm{eff}}}{d\rho_{\mathrm{eff}}} = \frac{\frac{4}{3}\Omega_{\gamma,0}(1+z) - \frac{n-3}{3} n \Omega_{n,0}(1+z)^{n-3}}{3\Omega_{\mathrm{b},0} + 4\Omega_{\gamma,0}(1+z) - n\Omega_{n,0}(1+z)^{n-3}}. \tag{35}$$

The properties of the bouncing term $\Omega_{n,0}$ are unknown. In particular, we do not know whether it influences the sound velocity. But we assume that sound can propagate in it as well as in baryonic matter and photons. Let us note that, with the lack of the bouncing term (i.e. $\Omega_{n,0} = 0$) and/or when sound does not propagate in the bouncing fluid, we obtain the standard formula for c_{s}^2 [28].

Knowing the acoustic scale we can determine the location of the mth peak

$$\ell_m \sim \ell_A (m - \phi_m) \tag{36}$$

where ϕ_m is the phase shift caused by the plasma driving effect. Assuming that $\Omega_{\mathrm{m},0} = 0.3$, on the surface of last scattering z_{dec} it is given by

$$\begin{aligned} \phi_m \sim 0.267 \left[\frac{r(z_{\mathrm{dec}})}{0.3}\right]^{0.1} &= 0.267 \left[\frac{1}{0.3}\frac{\rho_{\mathrm{r}}(z_{\mathrm{dec}})}{\rho_{\mathrm{m}}(z_{\mathrm{dec}})}\right]^{0.1} \\ &= 0.267 \left[\frac{1}{0.3}\frac{\Omega_{\mathrm{r},0}(1+z_{\mathrm{dec}})}{0.3}\right]^{0.1}, \end{aligned} \tag{37}$$

where $\Omega_{\mathrm{b},0}h^2 = 0.02$, and $r(z_{\mathrm{dec}}) \equiv \rho_{\mathrm{r}}(z_{\mathrm{dec}})/\rho_{\mathrm{m}}(z_{\mathrm{dec}}) = \Omega_{\mathrm{r},0}(1+z_{\mathrm{dec}})/\Omega_{\mathrm{m},0}$ is the ratio of the radiation to matter densities at the surface of the last scattering.

The locations of the first two peaks are taken from the CMB temperature angular power spectrum [42,43], while the location of the third peak is from the BOOMERANG measurements [44]. The values with uncertainties on the level 1σ are the following:

$$\ell_1 = 220.1^{+0.8}_{-0.8}, \qquad \ell_2 = 546^{+10}_{-10}, \qquad \ell_3 = 845^{+12}_{-25}.$$

From the WMAP data, only the Hubble constant is $H_0 = 72$ km/s MPc (or the parameter $h = 0.72$), the baryonic matter density $\Omega_{\mathrm{b},0} = 0.024h^{-2}$, and the matter density $\Omega_{\mathrm{m},0} = 0.14h^{-2}$ [42] which give a good agreement with the observation of the position of the first peak.

TABLE VIII. Values of $\Omega_{n,0}$ and location of first three peaks.

Model	Hubble constant	$\Omega_{n,0}$	ℓ_1	ℓ_2	ℓ_3
Extended bouncing model $n = 4$	$H_0 = 65$ km/s MPc	3.0×10^{-4}	217	517	816
	$H_0 = 72$ km/s MPc	2.86×10^{-4}	222	526	829
Extended bouncing model $n = 6$	$H_0 = 65$ km/s MPc	1.4×10^{-10}	223	530	847
	$H_0 = 72$ km/s MPc	1.3×10^{-10}	224	530	847

In the analysis of the constraints on the bouncing cosmological model parameters we fix the baryonic matter density $\Omega_{\mathrm{b},0} = 0.05$, the spectral index for initial density perturbations $n = 1$, and the radiation density parameter [28]

$$\Omega_{\mathrm{r},0} = \Omega_{\gamma,0} + \Omega_{\nu,0} = 2.48h^{-2} \times 10^{-5} + 1.7h^{-2} \times 10^{-5} = 4.18h^{-2} \times 10^{-5}, \quad (38)$$

which is a sum of the photon $\Omega_{\gamma,0}$ and neutrino $\Omega_{\nu,0}$ densities.

Assuming $\Omega_{\mathrm{m},0} = 0.3$ and $h = 0.72$, we obtain for the standard ΛCDM cosmological model the following positions of peaks:

$$\ell_1 = 220, \qquad \ell_2 = 521, \qquad \ell_3 = 821$$

with the phase shift ϕ_m given by (37).

From the SNIa data analysis, it was found that the Hubble constant has a lower value. Assuming that $H_0 = 65$ km/s MPc (or $h = 0.65$), we have $\Omega_{\mathrm{r},0} = 9.89 \times 10^{-5}$ from Eq. (38). For further calculations we take $\Omega_{\mathrm{r},0} = 0.0001$. If we consider the standard ΛCDM model, with $\Omega_{\mathrm{m},0} = 0.3$, $\Omega_{\mathrm{b},0} = 0.05$, the spectral index for the initial density perturbations $n = 1$, and $h = 0.65$, where sound can propagate in baryonic matter and photons, we obtain the following locations of first three peaks:

$$\ell_1 = 225, \qquad \ell_2 = 535, \qquad \ell_3 = 847.$$

We note the difference between the observational and theoretical values in this case. We check whether the presence of the bouncing term $\Omega_{n,0}$ moves the locations of the peaks. We do not know whether it influences the sound velocity, but we assume that sound can propagate in it as well as in baryonic matter and photons.

To obtain the bounce, $n > 4$ is necessary because the presence of the radiation term is required by the physics of primordial plasma in the recombination epoch. From the location of the first peak we obtain he limit for the $\Omega_{n,0}$ term. In the case $n = 5$, with $H_0 = 72$ km/s MPc, we obtain that $\Omega_{n,0} < 2 \times 10^{-11}$ while for $n = 6$ we have that $\Omega_{n,0} < 2 \times 10^{-17}$.

Please note that the special case $n = 6$ was analyzed for both values $H_0 = 65$ km/s MPc and $H_0 = 72$ km/s MPc and the agreement with the observation of the location of the first peak was obtained, also for the nonzero values of the parameter $\Omega_{n,0}$ [30]. It means that both values of H_0 are allowed from the CMB constraints for the case $n = 6$. However, this value is of order 10^{-10}. The results of calculations of the peak locations and the values of the parameter $\Omega_{n,0}$ are presented in Table VIII. In the special case $n = 4$, the bounce term scales like radiation, the existing of the bounce requires $\Omega_{n,0} > \Omega_{r,0}$. In this case, we also obtain the agreement with the observation of the location of the first peak for the nonzero values of the parameter $\Omega_{n,0}$ (on the order of 3×10^{-4}).

Finally, we analyze the models in which we assume that sound can propagate only in baryonic matter and photons. With $H_0 = 72$ km/s MPc, in the case of $n = 5$, we obtain that $\Omega_{n,0} < 2.2 \times 10^{-8}$ while for $n = 6$ we have that $\Omega_{n,0} < 5 \times 10^{-14}$. For the special case $n = 4$ we have that $\Omega_{n,0} = 2.3 \times 10^{-4}$.

We have also calculated the age of the Universe in the ΛBCDM model. We find that the difference in the age of the Universe is smaller than 10 million years for all values of $\Omega_{n,0}$ admissible by the CMB peaks location. So this model is admissible by the test of the age of the OHReG objects.

V. CONSTRAINT FROM THE BBN

The observations of abundance of light elements are in good agreement with the prediction of the standard big-bang nucleosynthesis (BBN). It means that the BBN does not allow for any significant divergence from the standard expansion law, apart from the beginning of BBN to the present epoch. Therefore, any nonstandard terms included in the Friedmann equation should give only a negligible small change during the BBN epoch to render the nucleosynthesis process unchanged.

It is crucial for the bouncing models to be consistent with BBN. These models have the nonstandard term Ω_n which scales like a^{-n} where $n > 4$. For example we analyze the cases $n = 5$ and $n = 6$. This additional term scales like $(1 + z)^n$. It is clear that such a term gives rise to the accelerated Universe expansion if $\Omega_{n,0} > 0$. Going backwards in time, this term would become dominant at some redshift. If it happened before the BBN epoch then the radiation domination would never occur and all BBN predictions would be lost.

The domination of the bouncing term Ω_n should end before the BBN epoch starts, and we assume that the BBN results are preserved in the bouncing models. In this way we obtain another constraint on the value of $\Omega_{n,0}$. Let the

TABLE IX. The value of z_{bounce} for the models under consideration: Einstein-de Sitter model (CDM), ΛCDM model (ΛCDM), bouncing model (BM), bouncing model with dust $m = 3$ (BCDM), and extended bouncing model with dust $m = 3$ (ΛBCDM).

Model	z_{bounce}
CDM	...
ΛCDM	...
BM	3.54×10^4
BCDM	2.98
BCDM with $n = 4$	3
BCDM with $n = 6$	4.05×10^4
ΛBCDM	∞
ΛBCDM with $n = 4$	∞
ΛBCDM with $n = 6$	∞

model modification be negligibly small during the BBN epoch and the nucleosynthesis process be unchanged. It means that the contribution of the bouncing term $\Omega_{n,0}$ cannot dominate over the radiation term $\Omega_{\text{r},0} \approx 10^{-4}$ before the BBN ($z \simeq 10^8$)

$$|\Omega_{n,0}|(1+z)^n < \Omega_{\text{r},0}(1+z)^4.$$

It means that $|\Omega_{n,0}| < 10^{-20}$ for the case $n = 6$ while $|\Omega_{n,0}| < 10^{-12}$ for the case $n = 5$, respectively. Of course, the case $n = 4$ is excluded because the existence of bouncing requires in this case $|\Omega_{n,0}| > \Omega_{\text{r},0}$, while BBN constraints require $|\Omega_{n,0}| < \Omega_{\text{r},0}$. Let us note that inequality $x_b \leq (\frac{|\Omega_{n,0}|}{\Omega_{r,0}})^{1/(n-4)}$ constrains the minimal size of the universe. The general conclusion from BBN constraints is that in the present epoch, the bouncing term, if it exists, is insignificant in comparison to the matter term.

Table IX gives the value of z_{bounce} calculated for the best-fitted model parameters. Because the bounce should take place before BBN epoch so z_{bounce} is greater than $z_{\text{BBN}} \simeq 10^8$. Comparing with the z_{bounce} presented in Table IX, we obtain that only two classes of models ΛCDM and ΛBCDM are admissible.

VI. CONCLUSION

In this paper we confront the bouncing model with astronomical observations. We use the constraints from SNIa data, CMB analysis, and BBN and the age of the oldest high-redshift objects.

The standard bouncing model is excluded statistically at the 4σ level. If we take the extended bouncing model (with extra $\Omega_{\Lambda,0}$ term) then we obtain, as the best fit, that the parameter $\Omega_{n,0}$ is equal to zero which means that the SNIa data do not support the existence of the bouncing term in the model. We also demonstrate that BBN gives stringent constraints on the extra term $\Omega_{n,0}$ and show that the bounce term is insignificant in the present epoch.

It is interesting that such bouncing models with extra inflationary expansion are presently favored in the loop quantum approach [45–48]. The theory of loop quantum gravity predicts that there is no initial singularity because of the quantum effects in the Planck scale. It is due to the continuum break and granularity of spacetime. Therefore, we consider the model where we assume a small positive value of $\Omega_{n,0}$ and estimate the rest of the parameters. This model is statistically admissible. However, when we compare this model with the standard ΛCDM model applying the Akaike criterion, the latter is preferred.

If the energy density is so large then quantum gravity corrections are important at both the big bang and big rip. It is interesting that the classical theory reveals its own boundaries (i.e. classical singularities). The account of quantum effect avoids not only an initial singularity but allows also to escape from a future singularity [49–51].

The avoidance of the initial singularity arises only on the quantum ground because the classical theory of gravity according to the Hawking-Penrose theorems states that these singularities are essential if only some reasonable conditions on the matter content are fulfilled.

If we assume the classical gravity is obvious during the whole evolution of the Universe then there is no reason to introduce the bouncing era. The ΛCDM model with the big bang is a simpler model, while the bouncing model requires the admittance of observationally unconfirmed assumptions. In this way Occam's razor methodology rules out the generalized bouncing model. The general conclusion is that the present astronomical data do not support the bouncing cosmology.

We also adopt the methods of dynamic systems for investigating dynamics in the phase space. The advantages of these methods are that they offer the possibility of the investigation of all evolutional paths for all initial conditions. We show that the dynamics can be reduced to a two-dimensional Hamiltonian system. We also show structural instability of both the standard and generalized bouncing models. Let us note that the concordance ΛCDM models are structurally stable [52]. The structural stability is a reasonable condition which should be satisfied by models of real physical processes. From the dynamic investigation, we obtain that all models with the bounce are rather fragile. It means that any small perturbation of the right-hand sides of the dynamic equations of the model changes the topological structure of the phase space. The bouncing models in the space of all dynamic systems on the plane form nondense (zero measure) subsets of this plane following the Peixoto theorem. Therefore, the bouncing models are untypical while ΛCDM models are generic from the point of view of structural stability.

ACKNOWLEDGMENTS

The paper was supported by KBN Grant No. 1 P03D 003 26.

[1] O. Lahav and A. R. Liddle, astro-ph/0406681.
[2] A. G. Riess *et al.* (Supernova Search Team), Astron. J. **116**, 1009 (1998).
[3] S. Perlmutter *et al.* (Supernova Cosmology Project), Astrophys. J. **517**, 565 (1999).
[4] P. J. E. Peebles and B. Ratra, Rev. Mod. Phys. **75**, 559 (2003).
[5] Z.-H. Zhu and M.-K. Fujimoto, Astrophys. J. **585**, 52 (2003).
[6] S. Sen and A. A. Sen, Astrophys. J. **588**, 1 (2003).
[7] D. Puetzfeld and X.-L. Chen, Classical Quantum Gravity **21**, 2703 (2004).
[8] T. Padmanabhan and T. R. Choudhury, Mon. Not. R. Astron. Soc. **344**, 823 (2003).
[9] T. R. Choudhury and T. Padmanabhan, Astron. Astrophys. **429**, 807 (2005).
[10] M. P. Dabrowski, W. Godlowski, and M. Szydlowski, Int. J. Mod. Phys. D **13**, 1669 (2004).
[11] W. Godlowski and M. Szydlowski, Gen. Relativ. Gravit. **36**, 767 (2004).
[12] W. Godlowski, M. Szydlowski, and A. Krawiec, Astrophys. J. **605**, 599 (2004).
[13] W. Godlowski, J. Stelmach, and M. Szydlowski, Classical Quantum Gravity **21**, 3953 (2004).
[14] W. Godlowski and M. Szydlowski, Gen. Relativ. Gravit. **35**, 2171 (2003).
[15] B. Feng, X.-L. Wang, and X.-M. Zhang, Phys. Lett. B **607**, 35 (2005).
[16] R. C. Tolman, *Relativity Thermodynamics and Cosmology* (Oxford University Press, Oxford, 1934).
[17] H. P. Robertson, Rev. Mod. Phys. **5**, 62 (1933).
[18] A. Einstein, Berl. Ber. **235** (1931).
[19] R. C. Tolman, Phys. Rev. **38**, 1758 (1931).
[20] P. J. Steinhardt and N. Turok, Nucl. Phys. Proc. Suppl. **124**, 38 (2003).
[21] Y. Shtanov and V. Sahni, Classical Quantum Gravity **19**, L101 (2002).
[22] D. H. Coule, Classical Quantum Gravity **22**, R125 (2005).
[23] J. M. Salim, S. E. Perez Bergliaffa, and N. Souza, Classical Quantum Gravity **22**, 975 (2005).
[24] N. Pinto Neto, Int. J. Mod. Phys. D **13**, 1419 (2004).
[25] J. D. Barrow, D. Kimberly, and J. Magueijo, Classical Quantum Gravity **21**, 4289 (2004).
[26] C. Molina-Paris and M. Visser, Phys. Lett. B **455**, 90 (1999).
[27] B. K. Tippett and K. Lake, gr-qc/0409088.
[28] R. G. Vishwakarma and P. Singh, Classical Quantum Gravity **20**, 2033 (2003).
[29] M. Szydlowski and A. Krawiec, Phys. Rev. D **70**, 043510 (2004).
[30] A. Krawiec, M. Szydlowski, and W. Godlowski, Phys. Lett. B **619** 219 (2005).
[31] M. Szydlowski, J. Szczesny, and T. Stawicki, Classical Quantum Gravity **5**, 1097 (1988).
[32] M. Szydlowski, J. Szczesny, and M. Biesiada, Classical Quantum Gravity **4**, 1731 (1987).
[33] V. Gorini, A. Y. Kamenshchik, U. Moschella, and V. Pasquier, gr-qc/0403062.
[34] M. Biesiada, W. Godlowski, and M. Szydlowski, Astrophys. J. **622**, 28 (2005).
[35] U. Alam, V. Sahni, and A. A. Starobinsky, J. Cosmol. Astropart. Phys. 04 (2003) 002.
[36] C. L. Bennett *et al.*, Astrophys. J. Suppl. Ser. **148**, 1 (2003).
[37] A. G. Riess *et al.* (Supernova Search Team), Astrophys. J. **607**, 665 (2004).
[38] B. Ratra and P. J. E. Peebles, Phys. Rev. D **37**, 3406 (1988).
[39] A. R. Liddle, Mon. Not. R. Astron. Soc. **351**, L49 (2004).
[40] H. Akaike, IEEE Trans. Auto Control **19**, 716 (1974).
[41] B. Chaboyer and L. M. Krauss, Science **299**, 65 (2003).
[42] D. N. Spergel *et al.*, Astrophys. J. Suppl. Ser. **148**, 175 (2003).
[43] L. Page *et al.*, Astrophys. J. Suppl. Ser. **148**, 233 (2003).
[44] P. de Bernardis *et al.*, Astrophys. J. **564**, 559 (2002).
[45] M. Bojowald, Phys. Rev. Lett. **86**, 5227 (2001).
[46] M. Bojowald, Phys. Rev. Lett. **89**, 261301 (2002).
[47] M. Bojowald and K. Vandersloot, Phys. Rev. D **67**, 124023 (2003).
[48] A. Ashtekar and J. Lewandowski, Classical Quantum Gravity **21**, R53 (2004).
[49] S. Nojiri and S. D. Odintsov, Phys. Lett. B **595**, 1 (2004).
[50] E. Elizalde, S. Nojiri, and S. D. Odintsov, Phys. Rev. D **70**, 043539 (2004).
[51] S. Nojiri and S. D. Odintsov, Phys. Rev. D **70**, 103522 (2004).
[52] S. Smale, *The Mathematics of Time: Essays on Dynamical Systems, Economic Processes, and Related Topics* (Springer-Verlag, Berlin, 1980).